

**This PDF file includes:**

1. Experimental section.....	S2-8
2. Supplementary data.....	S10
Figure S1.....	S10
Figure S2.....	S11
Figure S3.....	S12
Figure S4.....	S13
Figure S5.....	S14
Figure S6.....	S15-16
Figure S7.....	S17
Figure S8.....	S18
Figure S9.....	S19
Figure S10.....	S20
Figure S11.....	S21
Figure S12.....	S22
Figure S13.....	S23
Figure S14.....	S24
Figure S15.....	S25
Figure S16.....	S26
Figure S17.....	S27
Figure S18.....	S28
Figure S19.....	S29
FigureS20.....	S30
FigureS21.....	S31
FigureS22.....	S32
Table S1.....	S33
3. Appendix I.....	S34
4. Reference.....	S35

## 1. Experimental Section.

### 1.1 Materials.

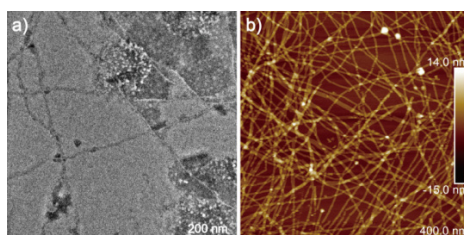
Hen egg white lysozyme (HEWL), bovine serum albumin (BSA), thioflavin T (ThT) and 8-anilino-1-naphthalenesulfonic acid (ANS) were purchased from Sigma-Aldrich. Tris(2-carboxyethyl) phosphine hydrochloride (TCEP) was purchased from TCI. Pig insulin and pepsin were purchased from Aladdin.  $\beta$ -lactoglobulin ( $\beta$ -Lg), ribonuclease A (RNase A), horseradish peroxidase (HRP), myoglobin and  $\alpha$ -lactalbumin ( $\alpha$ -La), cytochrome c (Cyt c) and  $\alpha$ -amylase were purchased from Yuanyebio Co., LTD. Ultrapure water was used in all experiments and supplied by Milli-Q Advantage A10 (Millipore, USA). The silicon wafer (Si) was purchased from Resemi Co., LTD. The silicon wafer was cleaned with Piranha solution (concentrated  $\text{H}_2\text{SO}_4$ : 35%  $\text{H}_2\text{O}_2$  = 7:3 v/v) at 80°C for 8 hrs.

#### 1.2.1 General strategy for the superfast amyloid-like assembly.

HEWL, BSA or  $\alpha$ -La were dissolved in Milli-Q water and insulin was dissolved in Milli-Q water at pH 3 (adjusted by HCl) with different concentrations. TCEP was dissolved in Milli-Q water (50 mM) with the pH being adjusted by NaOH (5 M). The reaction started from mixing equivoluminal solution of the protein and TCEP at room temperature.

#### 1.2.2 Formation of lysozyme fibrils in conventional amyloid aggregation.

HEWL solution (10 mg/ml) was incubated in aqueous (pH 2, adjusted by HCl) at 70°C for 7 days, and the lysozyme fibrils was visualized by AFM and TEM.



The lysozyme amyloid fibrils were prepared by conventional method. (a) The TEM image of nanofibrils; (b) the AFM image of nanofibrils.

### **1.3 Characterizations.**

Fluorescence spectrum was collected by F-7000 fluorescence spectrophotometer (Hitachi). Far-UV CD spectrum was collected by using Chirascan spectrophotometer (Applied Photophysics Ltd, England). Attenuated Total Reflectance Fourier Transform Infrared spectroscopy (ATR-FTIR) spectrum was recorded on a Vetex 70v (Bruker). For Transmission Electron Microscopy (TEM) analysis, JEM-2100 (JEOL, Japan) transmission microscopy with an acceleration voltage of 120 KV was utilized. Field Emission Scanning Electron Microscope (FE-SEM) observations were conducted on SU8020 (Hitachi) with an acceleration voltage of 1 KV and all the samples were without gold coating. Atomic Force Microscopy (AFM) was performed by Dimension Icon AFM (Bruker) in ScanAsyst mode and CSPM 5500 (MultiMode, NanoScope IV from Benyuan Inc, China) in Tapping mode. SDS-PAGE was performed in tricine buffer (pH 8.45) using a 8% stacking gel and a 16.5% separating gel. The bands of the gel were visualized by Coomassie brilliant blue R-250 staining. Raman spectrum was performed on inVia Reflex (Renishaw) with the 532 nm laser excitation being used. The surface tension measurements were carried out with Constrained Drop Surfactometry (CDS) developed by Zuo and coworkers.<sup>[1, 2]</sup>

#### **1.3.1 The quantification of disulfide bond by Raman spectrometer.**

5 ml lysozyme solution (10 mg/ml) mixed with 5 ml TCEP solution (pH 6.5, 5 mM), and 1 ml such sample was taken out from the mixed solution per every 1 minute and freeze-dried in liquid nitrogen at once. After the freeze-drying, the samples were characterized by Raman spectrometer. The content of disulfide (S-S) bond was calculated by quantifying the peak area ratio of S-S bond ( $505\text{ cm}^{-1}$ ) to the amide I band ( $1600\text{ cm}^{-1}$ - $1700\text{ cm}^{-1}$ ).<sup>[3]</sup>

#### **1.3.2 Thioflavin T (ThT) staining.**

100  $\mu\text{l}$  ThT solution (100  $\mu\text{M}$ ) mixed with 1 ml freshly prepared lysozyme (2

mg/ml), BSA (2 mg/ml),  $\alpha$ -La (1 mg/ml) or insulin (1 mg/ml) and incubated for 10 minutes in the cuvette. And then 1 ml TCEP solution (50 mM) with different pH was added to the cuvette, and the stained samples were then measured by the fluorescence spectrophotometer with the excitation at 440 nm and emission at 484 nm.

For the amyloid aggregation of lysozyme by conventional method, the lysozyme (2 mg/ml, pH 3, adjusted by HCl) was incubated at 75 °C, and 2 ml sample was taken out per every 10 minutes and stained by 100  $\mu$ l ThT solution (100  $\mu$ M), and the samples were then measured by the fluorescence spectrophotometer with the excitation at 440 nm and emission at 484 nm.

For the negative controls, 100  $\mu$ l ThT solution (100  $\mu$ M) mixed with 1 ml freshly prepared  $\beta$ -Lg (2 mg/ml), RNase A (2 mg/ml), Pepsin (2 mg/ml), HRP (2 mg/ml), Myoglobin (2 mg/ml), Cyt c (2 mg/ml) or  $\alpha$ -Amylase (2 mg/ml) and incubated for 10 minutes in the cuvette. And then 1 ml TCEP solution (50 mM) with pH 5.5 for  $\beta$ -Lg, pH 8.0 for RNase A, pH 2.0 for Pepsin, pH 8.0 for HRP, pH 7.0 for Myoglobin, pH 8.5 for Cyt c and pH 7.0 for  $\alpha$ -Amylase was added to the cuvette, and the stained samples were then measured by the fluorescence spectrophotometer with the excitation at 440 nm and emission at 484 nm.

Different pH may have an effect on ThT fluorescence intensity. It is reported that both acidic and basic pH would decrease significantly the intensity of ThT fluorescence intensity, and such pH-induced signal quenching is less in the presence of protein aggregates.<sup>[4]</sup> Accordingly, the overall effect of pH itself on the ThT fluorescence intensity in our system (protein aggregates) might be not so important to influence the curve tendency.

### **1.3.3 ANS staining.**

100  $\mu$ l ANS solution (100  $\mu$ M) mixed with 1 ml freshly prepared lysozyme (2 mg/ml), BSA (2 mg/ml),  $\alpha$ -La (1 mg/ml) or insulin (1 mg/ml) and incubated for 10 minutes in the cuvette. 1 ml TCEP solution (50 mM) with different pH was added to the cuvette, and the stained samples were then measured by the

fluorescence spectrophotometer with the excitation at 355 nm and emission at 470 nm.

For the amyloid aggregation of lysozyme by conventional method, the lysozyme (2 mg/ml, pH 3, adjusted by HCl) was incubated at 75 °C, and 2 ml sample was taken out per every 10 minutes and stained by 100  $\mu$ l ANS solution (100  $\mu$ M), and the samples were then measured by the fluorescence spectrophotometer with the excitation at 355 nm and emission at 470 nm.

For the negative controls, 100  $\mu$ l ANS solution (100  $\mu$ M) mixed with 1 ml freshly prepared the  $\beta$ -Lg (2 mg/ml), RNase A (2 mg/ml), Pepsin (2 mg/ml), HRP (2 mg/ml), Myoglobin (2 mg/ml), Cyt c (2 mg/ml),  $\alpha$ -Amylase (2 mg/ml) and incubated for 10 minutes in the cuvette. And then 1 ml TCEP solution (50 mM) with pH 5.5 for  $\beta$ -Lg, pH 8.0 for RNase A, pH 2.0 for Pepsin, pH 8.0 for HRP, pH 7.0 for Myoglobin, pH 8.5 for Cyt c and pH 7.0 for  $\alpha$ -Amylase was added to the cuvette, and the stained samples were then measured by the fluorescence spectrophotometer with the excitation at 355 nm and emission at 470 nm.

Different pH may have an effect on ANS fluorescence intensity. It is reported that only extremely acidic pH (e.g. pH<2) would enhance the intensity of ANS fluorescence intensity and shift the spectra (blue shift).<sup>[5]</sup> Obviously, in our cases with most pH values being higher than 3, the overall effect of pH itself on the ANS fluorescence intensity might be not so important to influence the curve tendency.

#### **1.3.4 Far-UV Circular Dichroism (CD) assay.**

1 ml lysozyme solution (1 mg/ml) mixed with 1 ml TCEP solution (20 mM, pH 5), 1 ml BSA solution (1 mg/ml) mixed with 1 ml TCEP solution (20 mM, pH 3), 1 ml  $\alpha$ -La solution (1 mg/ml) mixed with 1ml TCEP solution (20 mM, pH 3), 1 ml insulin solution (1 mg/ml) mixed with 1ml TCEP solution (20 mM, pH 3), due to requirement of the sample concentration for the far-UV CD spectrum, 100  $\mu$ l mixed solution diluted to 0.025mg/ml in 1 cm cuvette for CD assay, and

recorded from 200 nm to 260 nm with a 2.0 nm bandwidth. The content of second structure was calculated by CDNN (Applied Photophysics Ltd, England). Low pH and high dilution times ensured that there was no precipitation and consequent turbidity during the measurement, which then supported a relatively proper signal collection.

### **1.3.5 TEM assay.**

#### **For the nanofilm assembled by the oligomers at the air/water interface:**

50  $\mu$ l lysozyme solution (2 mg/ml) mixed with 50  $\mu$ l TCEP solution (50 mM, pH 7.5) and incubated for 2 hr on silicon wafer. By seriously transferring the silicon wafer with the solution covering the wafer surface into a tank with copious ultrapure water inside, the nanofilm was then floated on the surface of the ultrapure water. Detailed experimental description and video could be found in our previous work.<sup>[6]</sup> The nanofilm was taken out by copper grid, and characterized by TEM after drying and phosphotungstic acid staining.

**For the formation of the protofibrils:** the lysozyme (2 mg/ml) was treated with equivoluminal TCEP with pH 4.5 (50 mM), insulin was treated with equivoluminal TCEP with pH 3.0 (50 mM),  $\alpha$ -La was treated with equivoluminal TCEP with pH 3.0 (50 mM), BSA was treated with equivoluminal TCEP with pH 3.0 (50 mM). All samples were incubated at room temperature for 2 hr, and 100  $\mu$ l such sample was taken out and diluted to 5 ml. The copper grid (supported by carbon film) was immersed into the diluted sample and taken out after 5 seconds. The liquid drop was absorbed by a filter paper immediately and further negatively stained with 0.5-2% (w/v) phosphotungstic acid aqueous solution (pH 7.0) for about 5 min.

**For the assembly of the protofibrils in the bulk solution:** 1 ml lysozyme solution (1 mg/ml) mixed with 1 ml TCEP solution (50 mM, pH 6.5), and 100  $\mu$ l such sample was taken out at 1 min, 2 min, 4 min, 6 min and 10 min

respectively, and diluted to 5 ml by water. The copper grid (supported by carbon film) was immersed into the diluted sample and taken out after 5 seconds. The liquid drop was absorbed by a filter paper immediately and further negatively stained with 0.5-2% (w/v) phosphotungstic acid aqueous solution (pH 7.0) for about 5 min.

### **1.3.6 AFM assay on the nanofilm.**

50  $\mu$ l protein solution (2 mg/ml) mixed with 50  $\mu$ l TCEP solution (50 mM), the pH for insulin, lysozyme,  $\alpha$ -La and BSA is 4.5, 7.5, 5.0 and 4.5, respectively. After 8 hr incubation, by seriously transferring the silicon wafer with the solution covering on the wafer surface into a tank with copious ultrapure water inside, the nanofilm was then floated on the surface of the ultrapure water. Detailed experimental description and video could be found in our previous work.<sup>[4]</sup> The nanofilm was then taken out by silicon wafer and ultrasonically cleaned, and then dried at ambient conditions.

### **1.3.7 Molecular dynamics simulation.**

The X-ray diffraction structure of lysozyme (PDB: 5B1F) was used for this study. The reduced form of lysozyme was modeled without creating of Cys6-Cys127, Cys30-Cys115, Cys64-Cys80 and Cys76-Cys94 disulfide bond. A 200 ns molecular dynamics simulation of lysozyme and lysozyme without disulfide bonds were carried out with AMBER14 using the ff14SB and gaff force-field, and the hydrogen atoms were added to initial model using the leap module. All structures were immersed in cubic water boxes with at least 10 Å between the protein and the box boundary. The net charge of the system was neutralized with addition of counter ions.

Firstly, each system was energy minimized for 5000 steps with constraints on the protein using steepest descent method, followed by conjugated gradient method for 5000 steps full minimization without any constraints and then

warmed up from 0K to 310K. The temperature was regulated using Langevin dynamics temperature regulation. At last, MD simulation production continued 200 ns at temperature 310K and a pressure of 1 atm and pH 7. All bond lengths were constrained using the SHAKE algorithm. Snapshots were conserved once per 50 ps.

### 1.3.8 Constrained Drop Surfactometry (CDS)

The CDS is a newly developed single-droplet based experimental platform for characterizing interfacial reaction and self-assembly.<sup>[1,2]</sup> As shown in **Figure 2a** and **Figure S6a**, a sessile drop is constrained on a carefully machined pedestal that uses its knife-sharp edge to keep the drop integrity and to prevent film leakage even at low surface tensions. Real-time surface tension of the air/water interface is determined photographically from the shape of the droplet using axisymmetric drop shape analysis (ADSA).<sup>[1,2]</sup> The volume, surface area, and surface tension of the droplet are carefully manipulated and controlled with newly developed closed-loop ADSA.<sup>[2]</sup>

Here, the CDS was used to characterize the nanofilm adsorbed at the air/water interface resulted from the superfast amyloid-like assembly. A 40  $\mu$ L droplet of 0.5 mg/mL lysozyme solution at pH 5.5 was formed on a 5 mm pedestal in the CDS. The droplet was left undisturbed for 30 min to allow adsorption of the protein onto the air/water interface, indicated by decreasing surface tension with time (**Figure 2b** and **Figure S6b**). During this process, the volume of the droplet was maintained at constant using the closed-loop ADSA (**Figure S6b**). Subsequently, 4  $\mu$ L TCEP at 50 mM and pH 5.5 was injected into the lysozyme droplet using a microsyringe. The mixture of lysozyme and TCEP was incubated for 1 hr to allow sufficient mixing and reaction (**Figure 2c** and **Figure S6c**). To transfer the oligomer nanofilm adsorbed at the air/water interface using Langmuir-Blodgett (LB) transfer, residuals of the chemical reaction were carefully washed out from the droplet with buffer using a subphase replacement technique.<sup>[2]</sup> The subphase replacement was implemented using

a coaxial CDS pedestal through which the chemical residual was slowly withdrawn from the droplet and simultaneously replaced with an equal-quantity of buffer injected into the droplet. Consequently, the chemical residual in the droplet was washed out and replaced with the buffer while keeping a constant drop volume and without interfering with the adsorbed nanofilm at the air/water interface, indicated by the constant surface tension during the subphase replacement process (**Figure 2d** and **Figure S6d**). After the subphase replacement, the nanofilm adsorbed at the air/water interface was transferred onto a freshly peeled mica surface at a rate of 1 mm/min using an *in situ* LB transfer technique (**Figure S6e**). The transferred film was imaged with ScanAsyst mode AFM in air (**Figure S6e**).

## 2. Supplementary data.

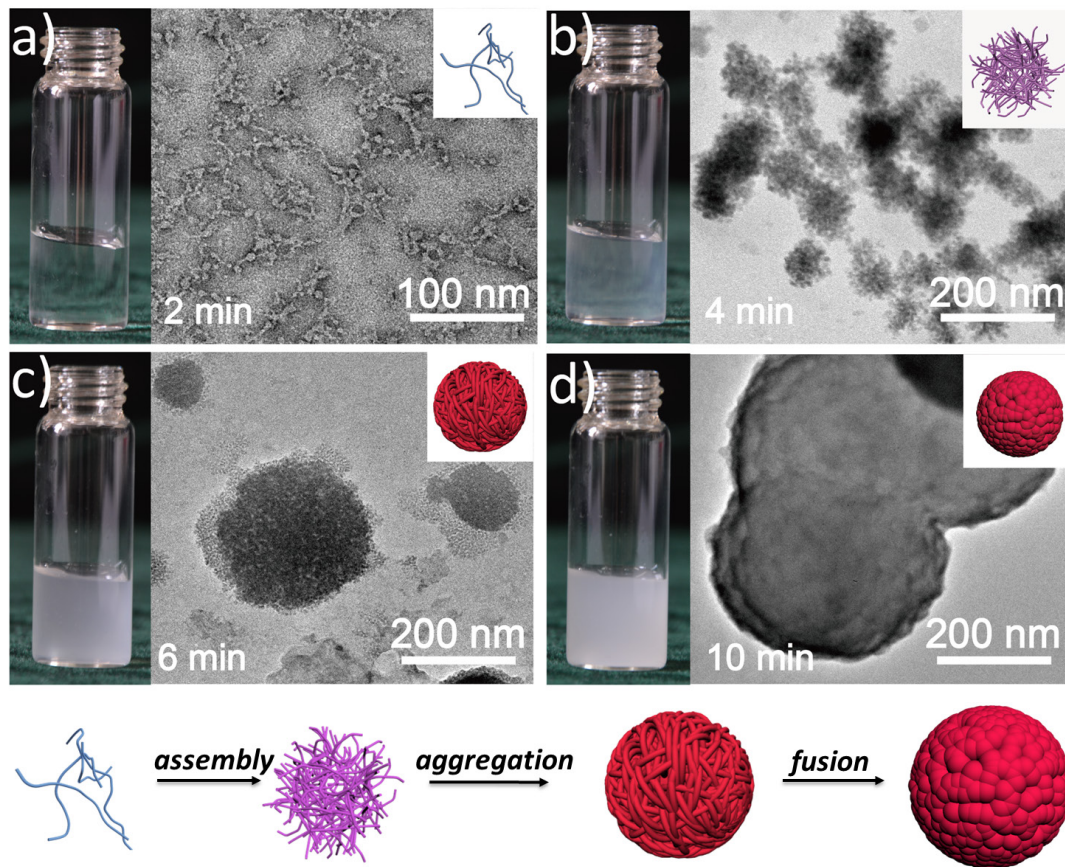


**Figure S1.** The assembly of protofibrils in the bulk solution (lysozyme 1 mg/ml, TCEP 50 mM, pH 6.5). (a) The protofibrils were observed in the bulk solution by TEM in 2 min; (b) the aggregation of the protofibrils in 4 min; (c) the aggregation of the protofibrils in 6 min; (d) the aggregation of the protofibrils in 10 min.

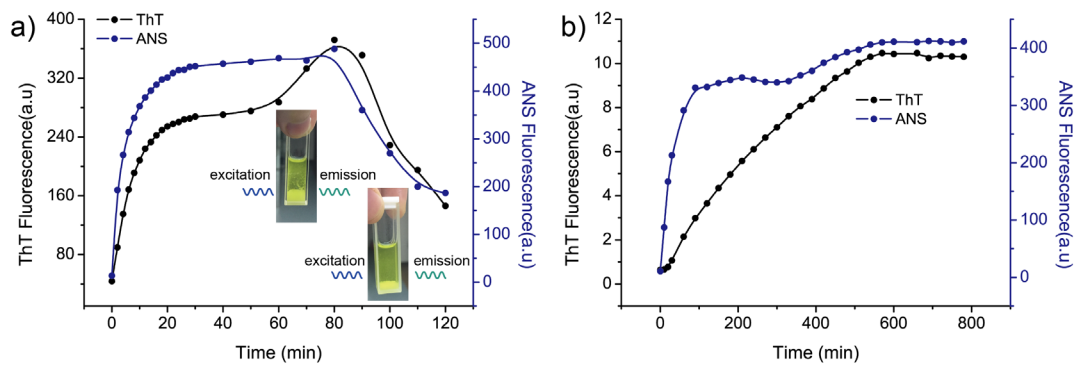


**Figure S2.** (a) The ThT and ANS fluorescence of lysozyme during the reduction of S-S bonds by TCEP at pH 7 (lysozyme 2 mg/ml, TCEP 50 mM, pH 7, room temperature). The ThT fluorescence increased again at 60 min because the aggregations enriched nearby the incident light that promoted the concentration of ThT. When the aggregation sank to bottom, the ThT and ANS fluorescence decreased rapidly after 80 min; (b) The ThT and ANS fluorescence of lysozyme during the reduction of S-S bonds by TCEP at pH 4 (lysozyme 2 mg/ml, TCEP 50 mM, pH 4, room temperature).

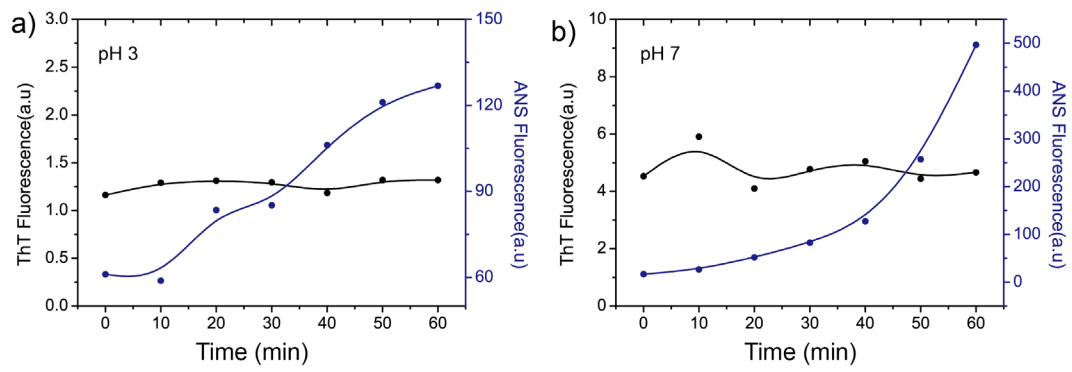


**Figure S3.** The ANS and ThT fluorescence of lysozyme in conventional amyloid aggregation process: (a) lysozyme 2 mg/ml, pH 3, 75 °C; (b) lysozyme 2 mg/ml, pH 7, 75 °C.

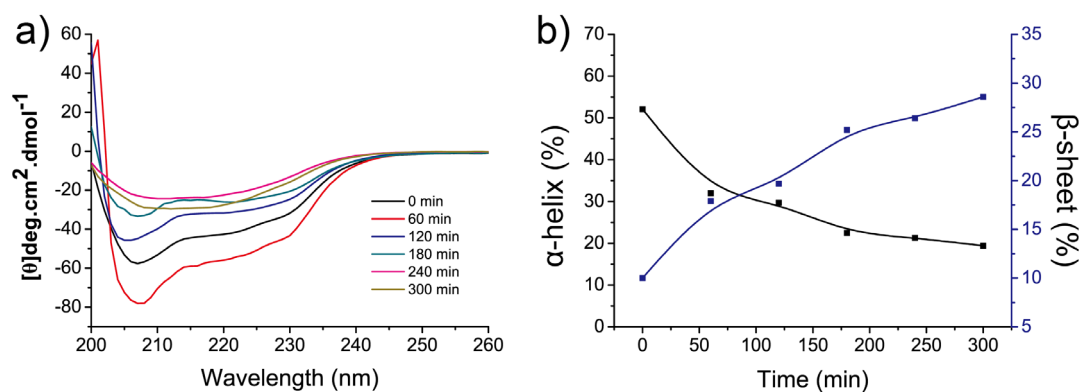


**Figure S4.** Circular dichroism (CD) characterization of lysozyme with treatment of TCEP (a) and the corresponding quantitative analysis (b). The successive loss at 223 and 208 nm indicated the loss of helix structure, and the negative peak around the 216 nm indicated the formation of  $\beta$ -sheet structure.

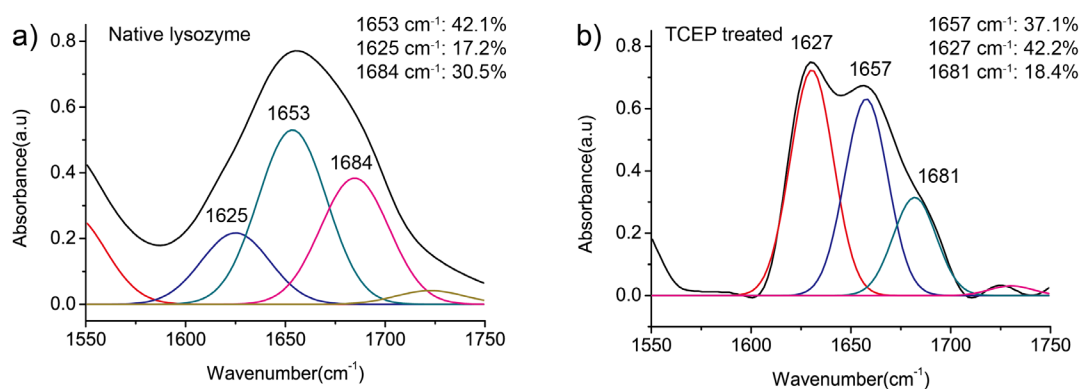


**Figure S5.** The deconvolution of amide I of native lysozyme (a) and TCEP treated lysozyme (2 mg/ml, TCEP 50mM, pH 7.5, 2 hr incubation). The peak around 1625 cm<sup>-1</sup> is attributed to  $\beta$ -sheet, the peak around 1655 cm<sup>-1</sup> is attributed to  $\alpha$ -helix and the peak around 1680 cm<sup>-1</sup> could be attribute to  $\beta$ -turns.

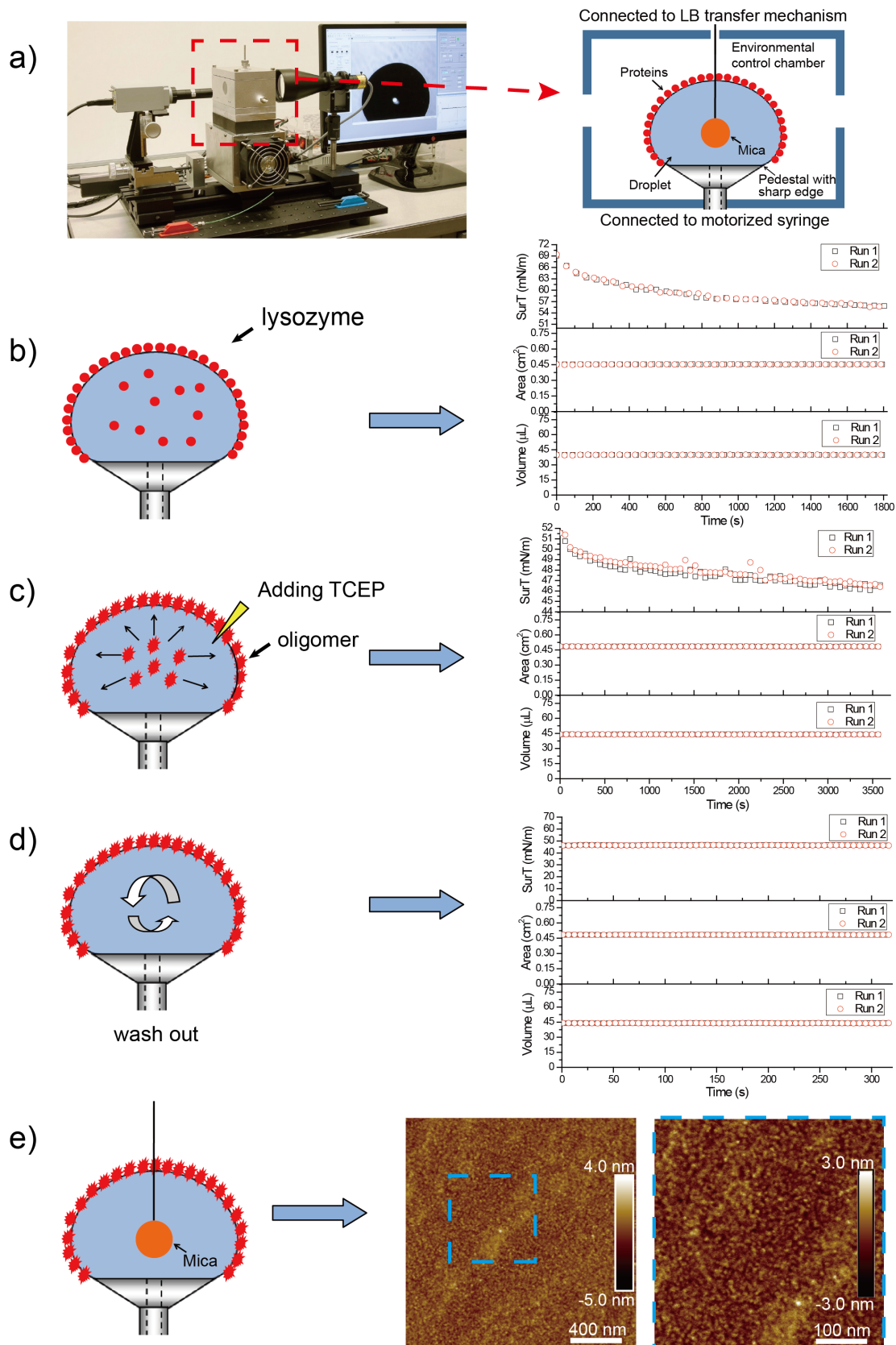


**Figure S6.** (a) The schematic of the constrained drop surfactometry (CDS) with the integrated Langmuir-Blodgett (LB) transfer mechanism; (b) a lysozyme solution droplet (40  $\mu\text{L}$ , 0.5 mg/mL, pH 5.5) was formed on a 5 mm

pedestal. Adsorption of the protein onto the air/water interface was monitored for 30 min, as indicated by surface tension decrease; (c) 4  $\mu$ L TCEP (50 mM, pH 5.5) was injected into the droplet, lysozyme and TCEP were mixed and incubated for 1 hr to allow sufficient reaction; (d) the chemical residual in the droplet was washed out with the HEPES buffer using a subphase replacement technique; during the subphase replacement process, the adsorbed nanofilm at the air/water interface remained intact as indicated by the constant surface tension; (e) the adsorbed nanofilm was transferred onto a mica surface using an *in situ* LB transfer technique, and imaged with AFM.

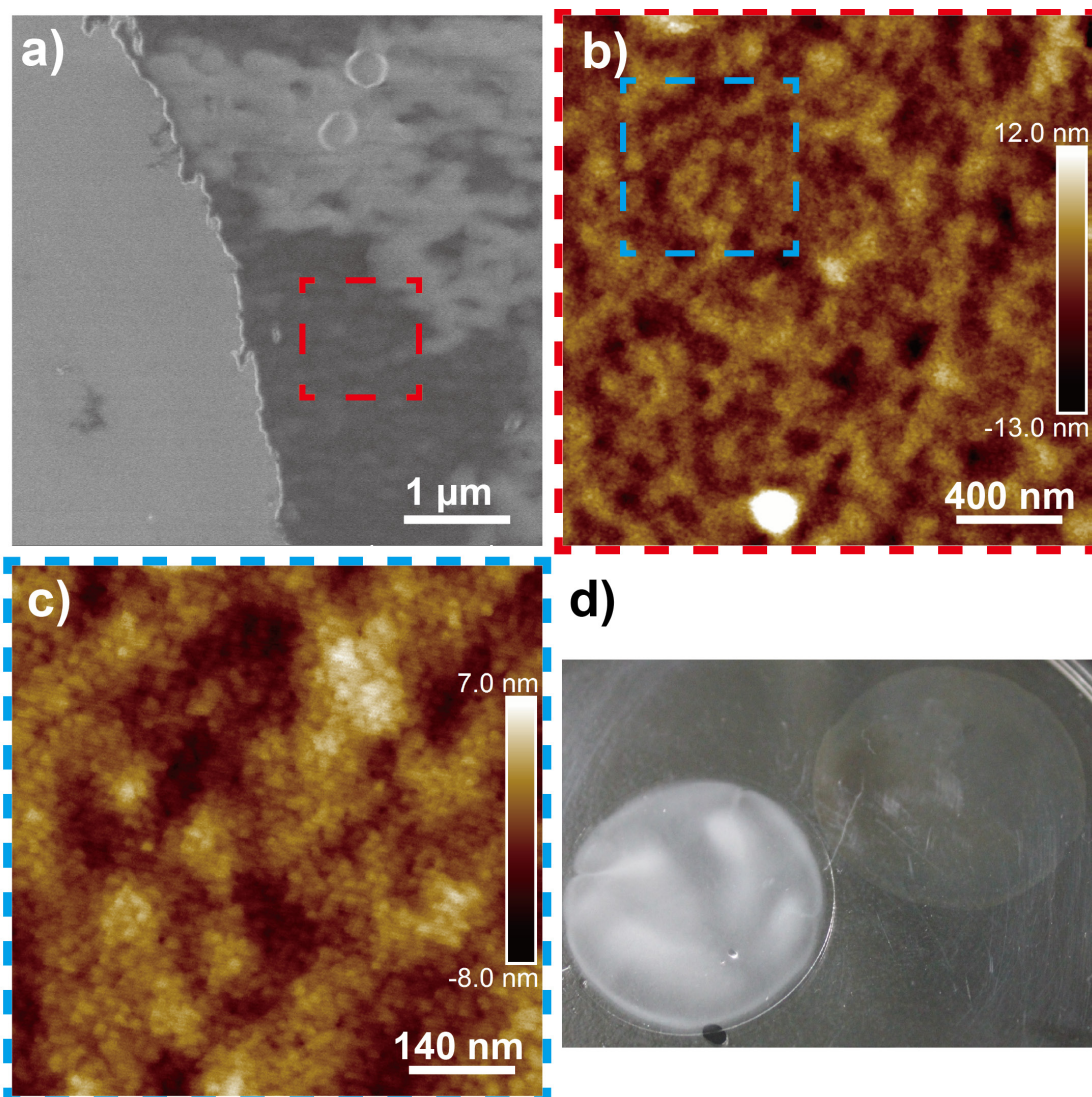


**Figure S7.** The SEM image (a) and AFM (b, c) images of lysozyme nanofilm at the air/water interface (lysozyme 2 mg/ml, 50 mM TCEP, pH 6.5, 1 hr incubation); (d) the photographic image of the nanofilm at air/water interface.

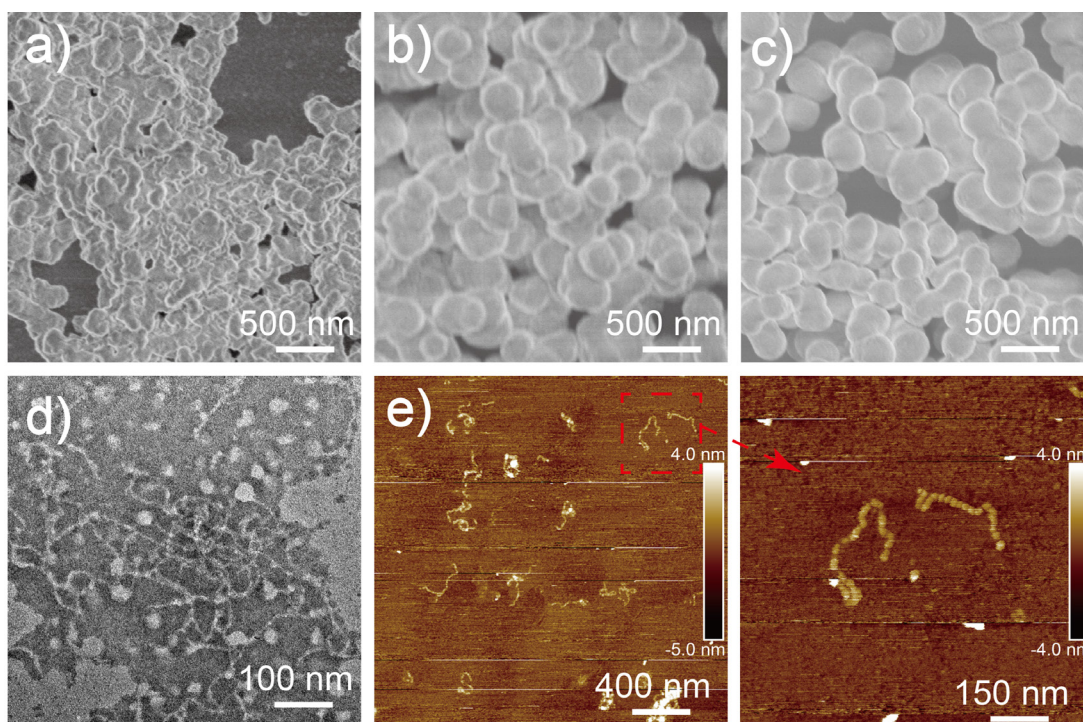


**Figure S8.** The SEM characterizations on lysozyme aggregations with different TCEP pH value (a) 6.5 (b) 7.5 (c) 8.5, the TEM image (d) and AFM (e) image of soluble protofibrils at pH 4.5.

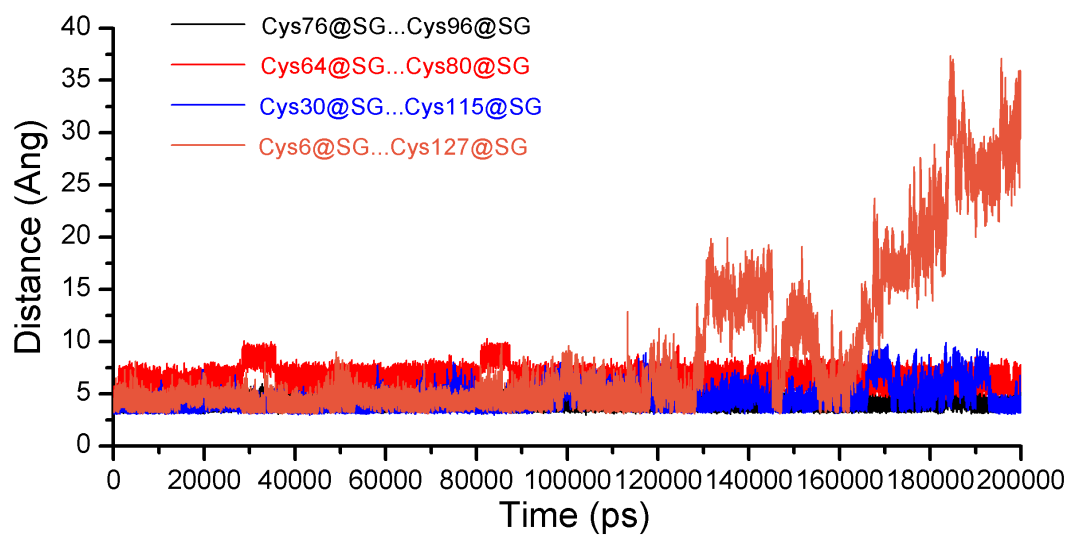


**Figure S9.** The distance changes of sulfur atoms in each broken disulfide bond.

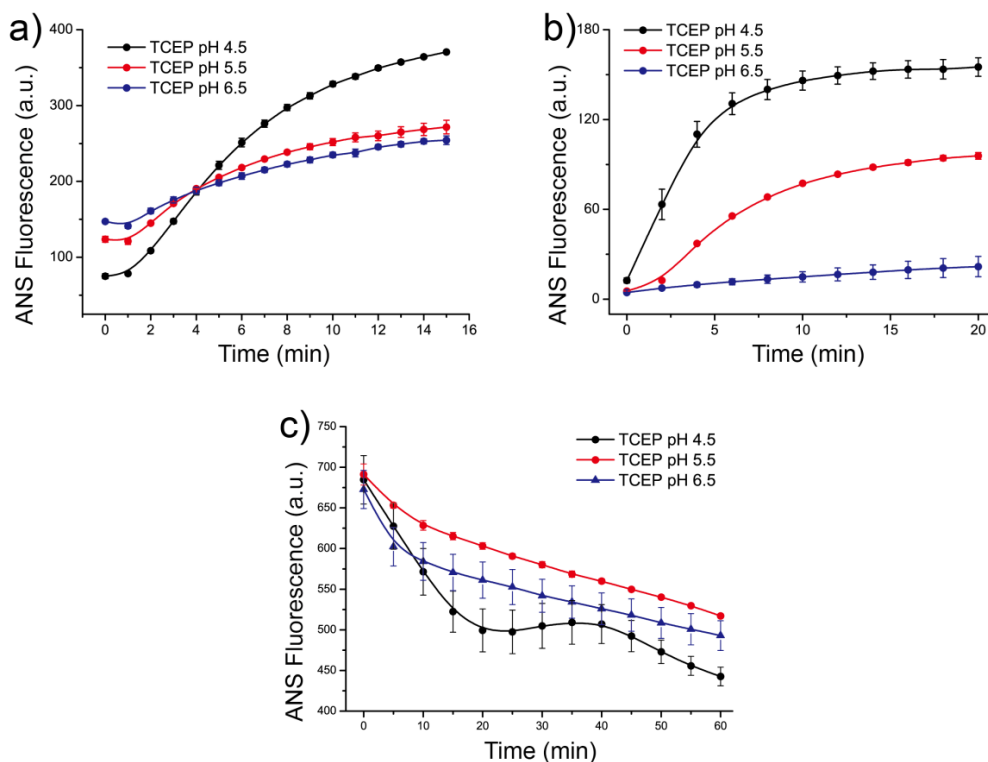


**Figure S10.** (a) ANS fluorescence of insulin with different pH of TCEP; (b) ANS fluorescence of  $\alpha$ -La with different pH of TCEP; (c) ANS fluorescence of BSA with different pH of TCEP. In the case of BSA, the decrease of ANS fluorescence is just because that unlike other protein used in the present work, BSA is a transport protein and has many binding sites for hydrophobic lipids or drugs that can also bind to ANS.<sup>[7]</sup> Various works have studied the binding properties of ANS to BSA, and revealed that the ANS could not only bind on the protein molecular surface, the binding sites but also locate at the hydrophobic cavities in BSA.<sup>[8, 9]</sup> Therefore, the saturation of ANS binding sites on BSA led to the maximal ANS fluorescence at the initial stage, and then the ANS fluorescence decreased with the disruption of native BSA structure and aggregation of the unfolded BSA induced by the superfast amyloid-like assembly. Such behavior was also similarly observed in the GnHCl-induced denaturation of human serum albumin (HSA).<sup>[10]</sup> In that study, the ANS fluorescence intensity with the drastic denaturation of HSA was lower than that of native HSA when the GnHCl was above 3 M, which indicated the unfolding of serum albumin led to the decrease of the ANS fluorescence.

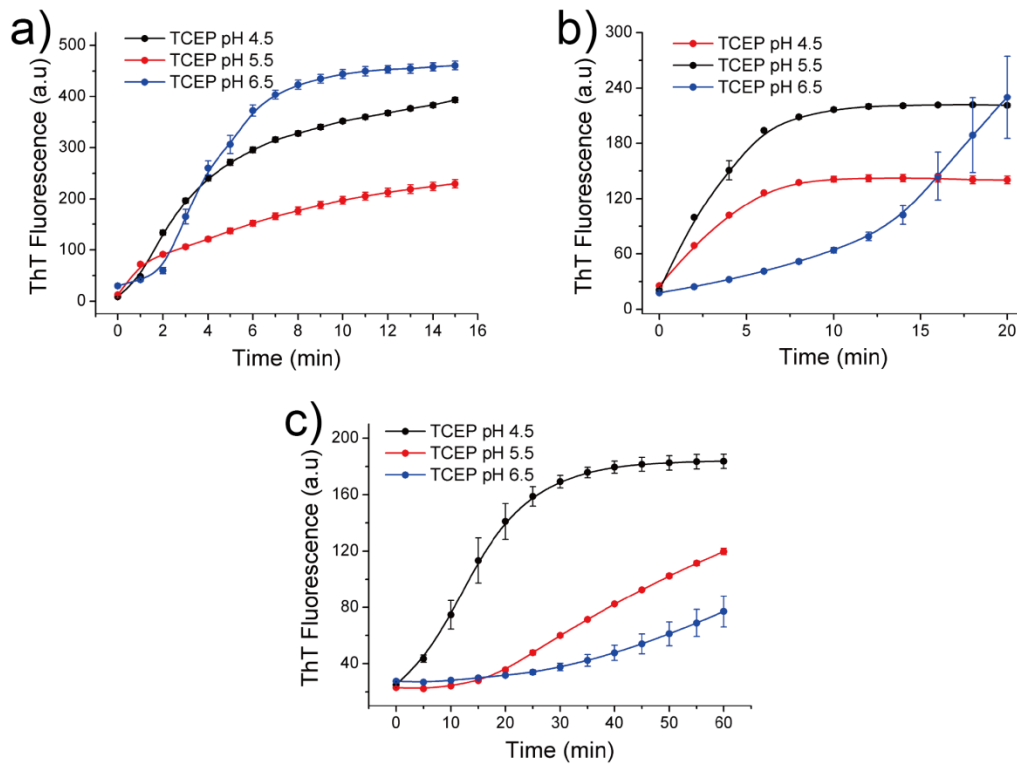


**Figure S11.** (a) ThT fluorescence of insulin with different pH of TCEP; (b) ThT fluorescence of  $\alpha$ -La with different pH of TCEP; (c) ThT fluorescence of BSA with different pH of TCEP.

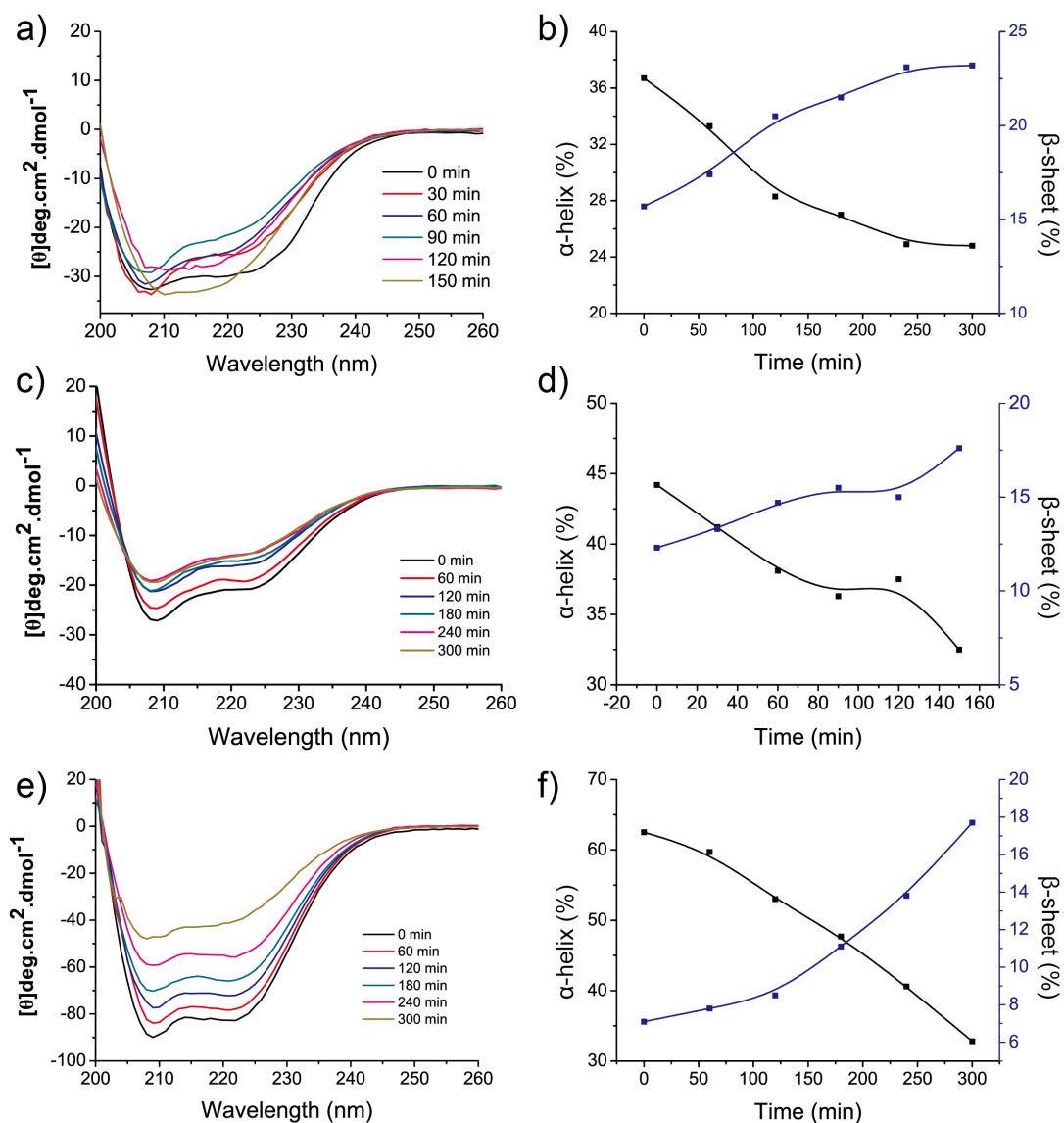


**Figure S12.** (a, b) Circular dichroism (CD) measurement of insulin with treatment of TCEP of pH 3; (c, d) CD measurement of  $\alpha$ -La with treatment of TCEP of pH 3; (e, f) CD measurement of BSA with treatment of TCEP of pH 3.

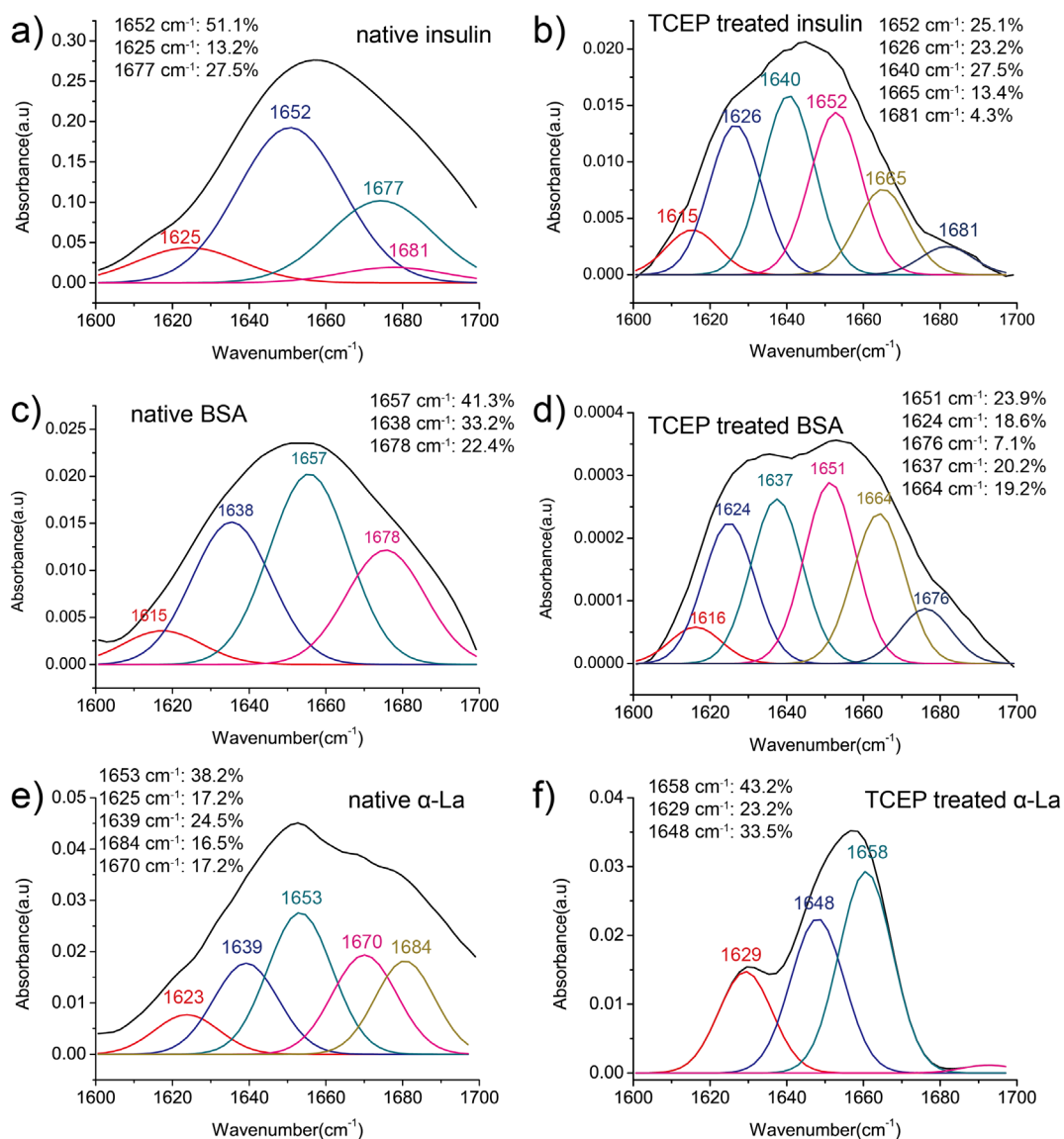


**Figure S13.** The IR characterization in amide I of native proteins and proteins with treatment of TCEP (the peak around 1625 cm<sup>-1</sup> is assigned to the  $\beta$ -sheet and the peak around 1655 cm<sup>-1</sup> is assigned to the  $\alpha$ -helix).

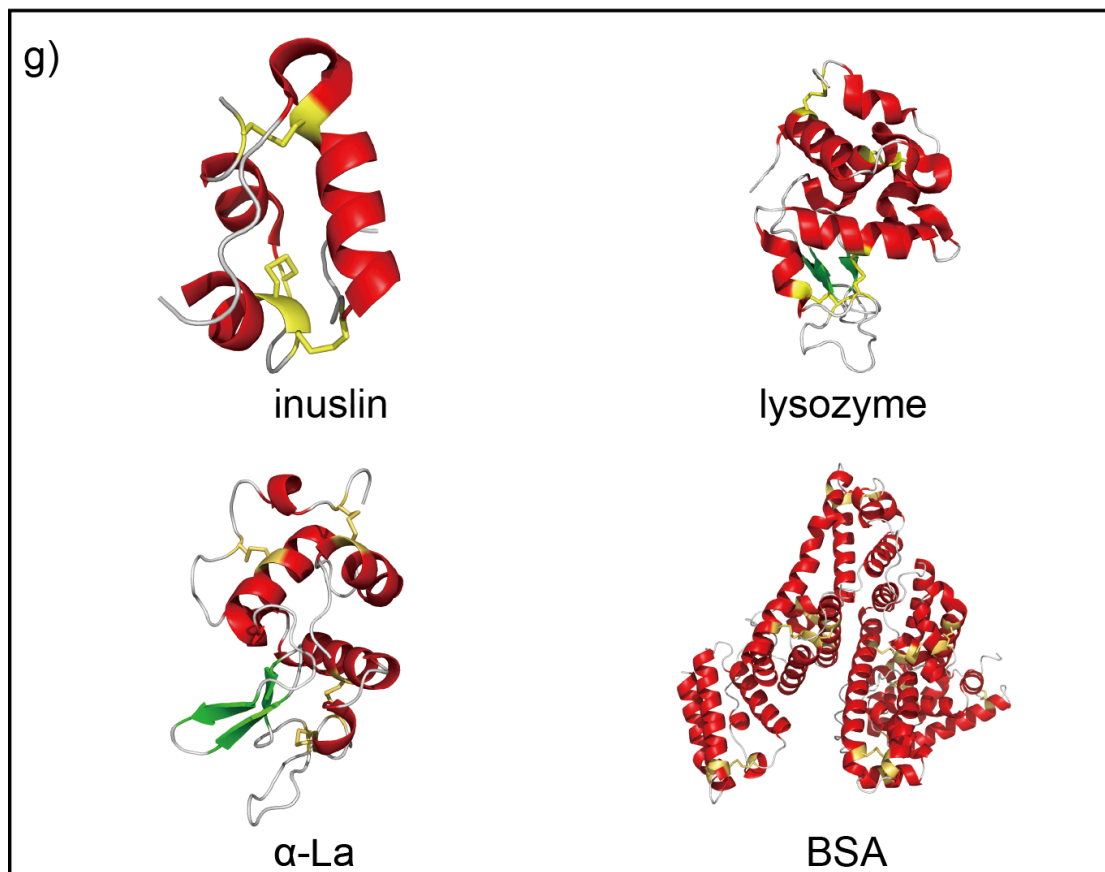
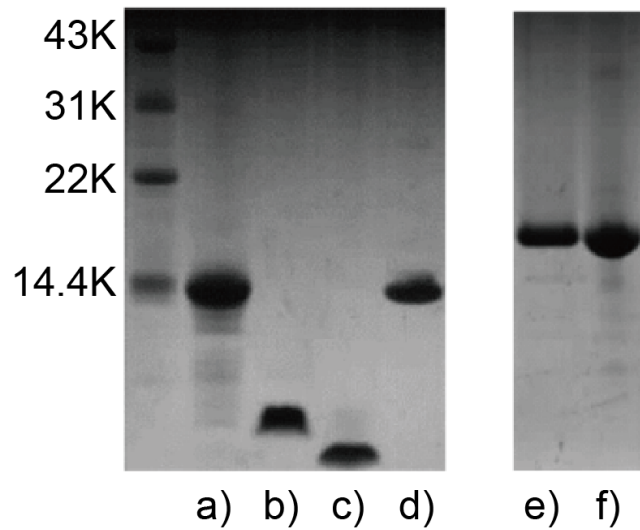


**Figure S14.** The SDS-PAGE of TCEP treated proteins (a-f): (a) TCEP treated lysozyme; (b) native insulin; (c) TCEP treated insulin: among all three disulfide bonds, the A-chain and B-chain were linked by two disulfide bonds in insulin, so that the molecular weight decreased with the treatment of TCEP; (d) TCEP treated  $\alpha$ -La; (e) native BSA; (f) TCEP treated BSA; (g) the S-S bonds shown by the yellow sticks in the proteins.

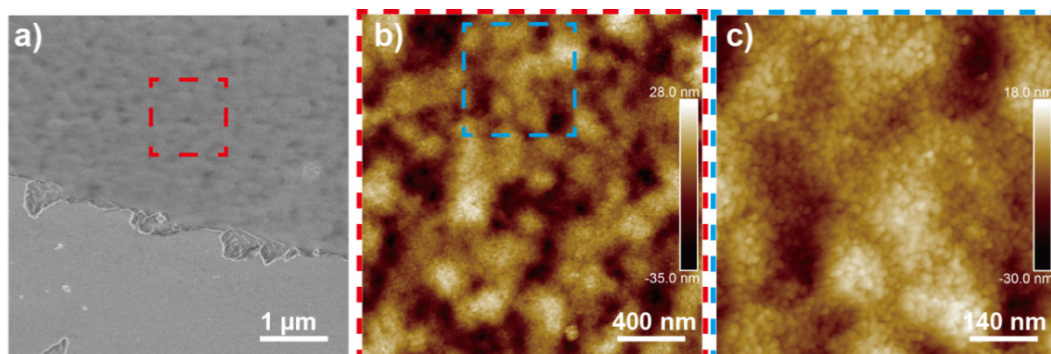


**Figure S15.** The SEM image (a) and AFM images (b, c) of insulin nanofilm at the air/water interface (insulin 2 mg/ml, 50 mM TCEP, pH 4.5, 2 hr incubation).

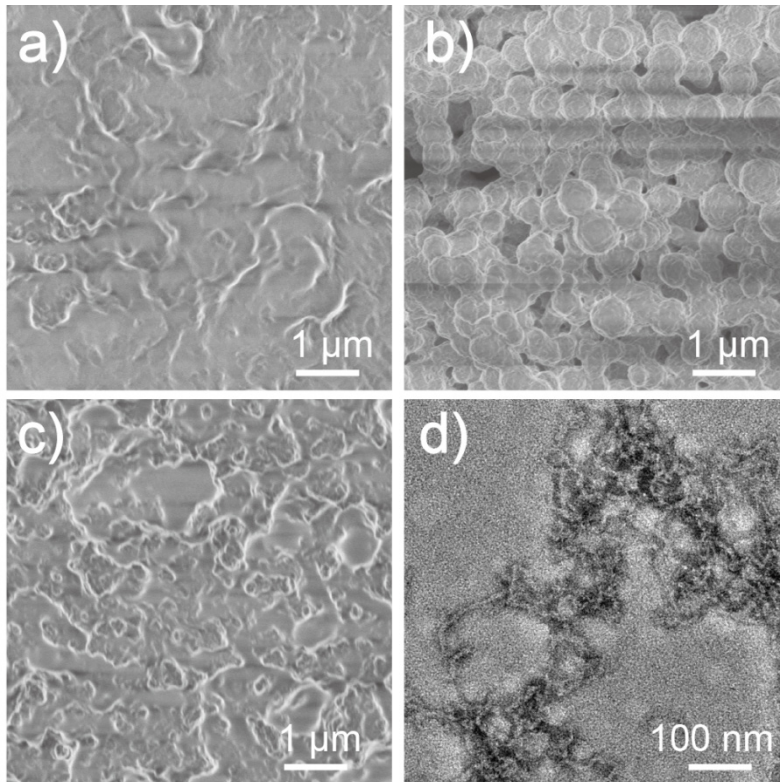


**Figure S16.** The SEM images of insulin aggregations with different TCEP pH value (a) 4.5, (b) 5.5, (c) 6.5, and the TEM image (d) of insulin protofibrils with TCEP pH of 3.

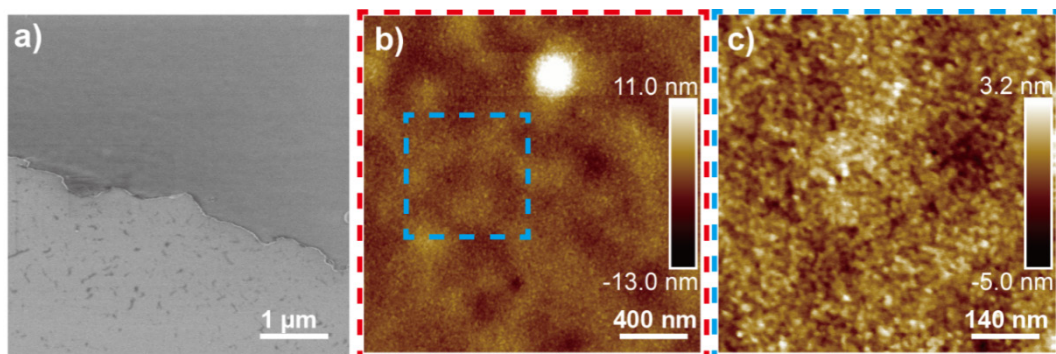


**Figure S17.** The SEM image (a) and AFM images (b, c) of  $\alpha$ -La nanofilm at the air/water interface ( $\alpha$ -La 2 mg/ml, 50 mM TCEP, pH 5.0, 2 hr incubation).

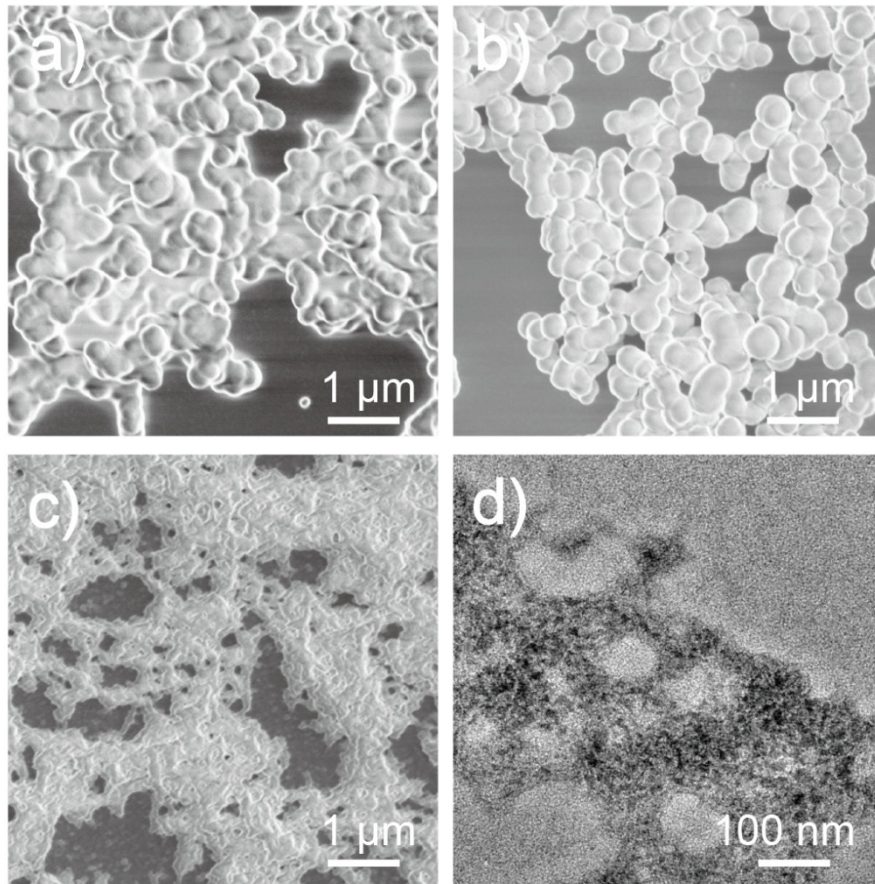


**Figure S18.** The SEM images of  $\alpha$ -La aggregations with different TCEP pH value (a) 4.5, (b) 5.5, (c) 6.5, and the TEM image (d) of  $\alpha$ -La protofibrils with TCEP pH of 3.

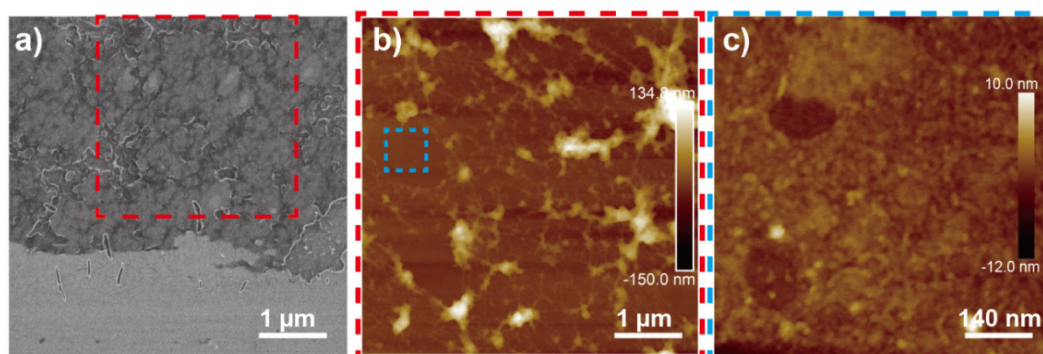


**Figure S19.** The SEM image (a) and AFM images (b, c) of BSA nanofilm at the air/water interface. The BSA nanofilm is thicker and rougher than the nanofilms of other proteins, because the relatively slower amyloid-like assembly process for BSA leads to the adsorption of the protofibrils from the bulk onto the nanofilm (BSA 2 mg/ml, 50 mM TCEP, pH 4.5, 5 hr incubation).

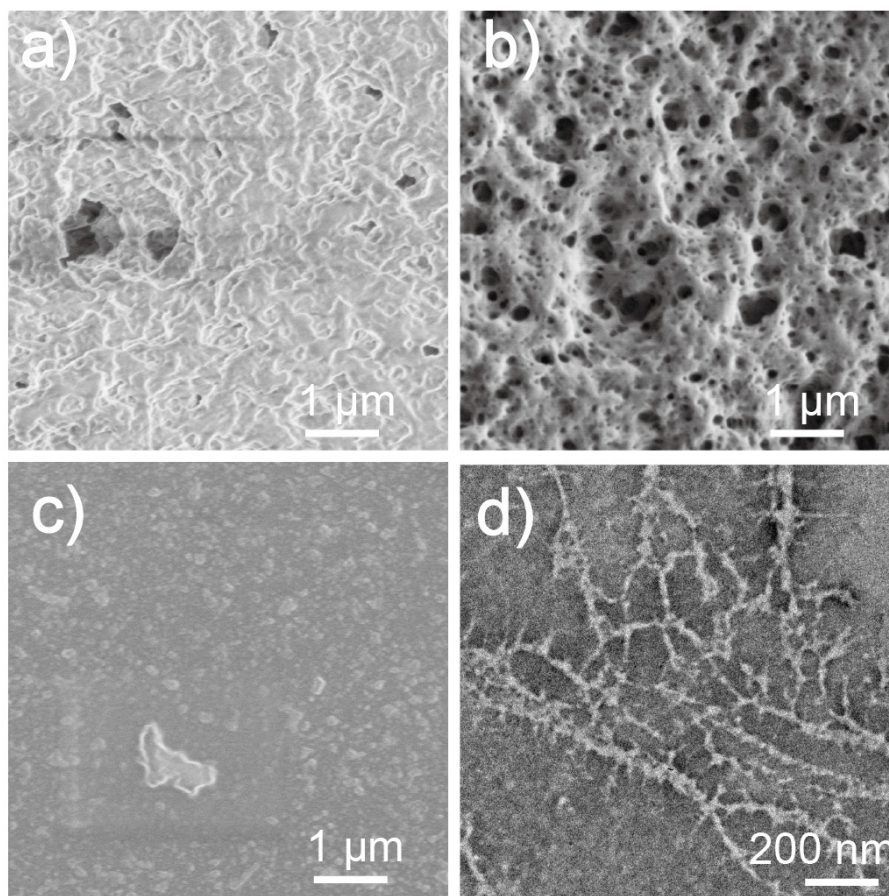


**Figure S20.** The SEM images of BSA aggregations with different TCEP pH value (a) 4.5, (b) 5.5, (c) 6.5, and the TEM image (d) of BSA protofibrils with TCEP pH of 3.

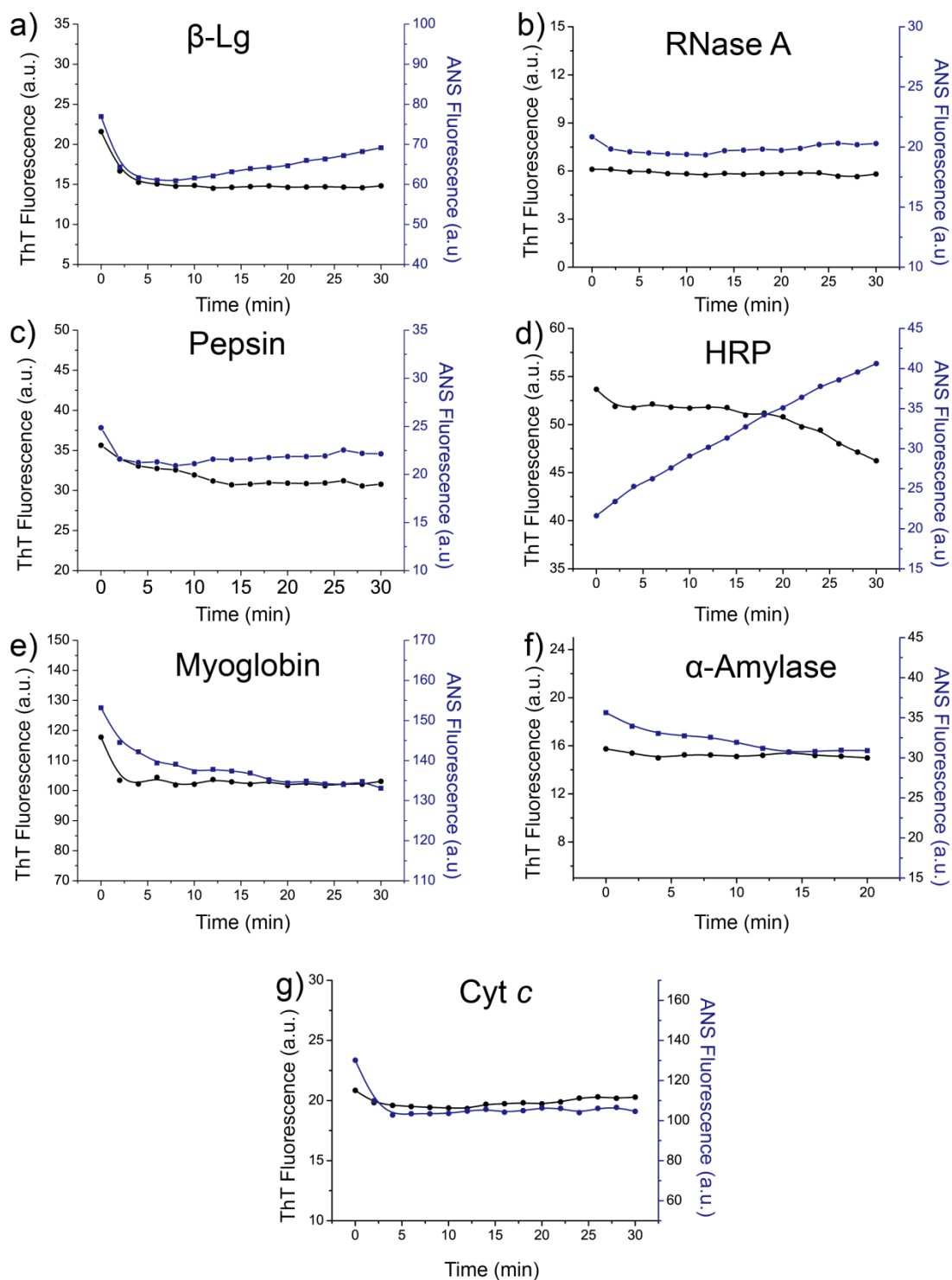


**Figure S21.** The ThT and ANS fluorescence of (a)  $\beta$ -Lg with treatment of TCEP of pH 5.5; (b) RNase A with treatment of TCEP of pH 8.0; (c) Pepsin with treatment of TCEP of pH 2.0; (d) HRP with treatment of TCEP of pH 8.0; (e) Myoglobin with treatment of TCEP of pH 7.0; (f)  $\alpha$ -Amylase with treatment of TCEP of pH 7.0; (g) Cyt c with treatment of TCEP of pH 8.5. *The fluorescence figures reflected that in the negative control samples, there was no obvious amyloid transition after mixing with TCEP.*

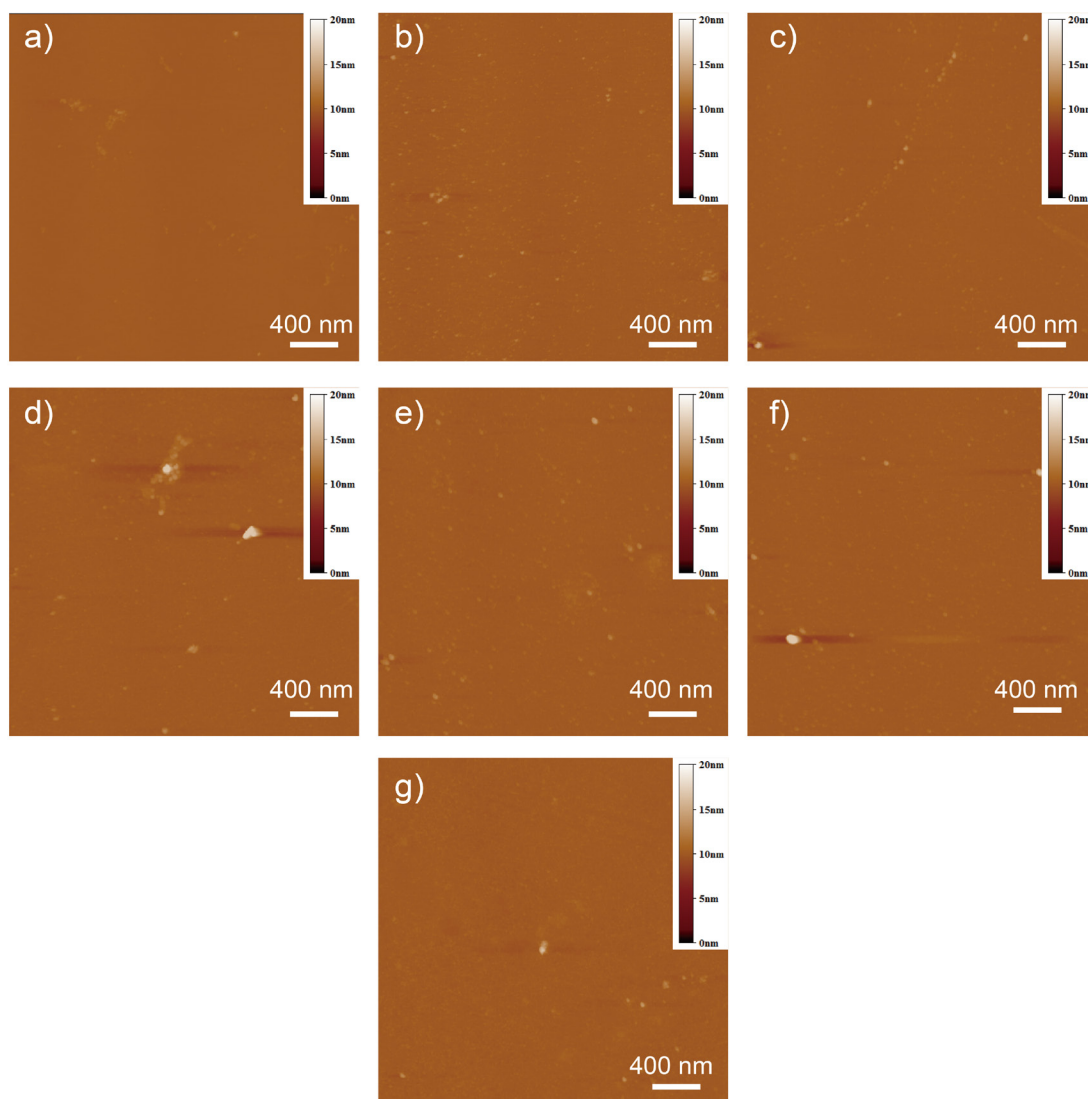


**Figure S22.** The AFM images of (a)  $\beta$ -Lg with treatment of TCEP of pH 5.5; (b) RNase A with treatment of TCEP of pH 8.0; (c) Pepsin with treatment of TCEP of pH 2.0; (d) HRP with treatment of TCEP of pH 8.0; (e) Myoglobin with treatment of TCEP of pH 7.0; (f)  $\alpha$ -Amylase with treatment of TCEP of pH 7.0; (g) Cyt c with treatment of TCEP of pH 8.5. *The AFM images clearly revealed that in the negative control samples, there was no obvious formation of oligomers, protofibrils or resultant nanofilms, microparticles after mixing with TCEP.*

For the negative controls, 1 ml freshly prepared protein solutions (2 mg/ml) were firstly mixed with 1 ml TCEP solution (50 mM). All samples incubated at room environment for 60 min. Then, the mixed solution was diluted 500 times, and 2  $\mu$ l diluted solution was dropped on mica and dried in room environment. The AFM images were then carried out by CSPM 5500 in Tapping mode.

**Table S1.** Different proteins for the control experiments.

	Proteins	S-S bonds	$\alpha$ -helix	$\beta$ -sheet	Fibrillation propensity	pI
Positive	HEWL	4	~54%	~6%	high	11.0
	Insulin	3	~51%	~0	high	5.5-6.0
	$\alpha$ -La	4	~35%	~6%	high	4.5-5.0
	BSA	17	~67%	~0	high	4.5-5.0
Negative	$\beta$ -Lg	2	~23%	~41%	high	5.1-5.3
	RNase A	4	~26%	~46%	high	8.6-9.4
	Cyt c	0	~47%	~10%	high	9.5-10.5
	$\alpha$ -Amylase	4	~31%	~14%	low	6.5-7.5
	Pepsin	3	~21%	~44%	low	1.0
	HRP	4	~60%	~2%	low	7.2-8.0
	Myoglobin	0	~83%	~0	high	6.8-7.2

The properties of proteins obtained from PBD. The secondary structure content was calculated by the residues numbers of secondary structure in full residues. PBD files (5B1F) for Lysozyme, (4f5s) for BSA, (5fb6) for Insulin, (1hfx) for  $\alpha$ -La, (3blg) for  $\beta$ -Lg, (1rnx) for RNase A, (3utl) for Pepsin, (2ylj) for HRP, (4twv) for Myoglobin, (1c52) for Cyt c and (1aqh) for  $\alpha$ -Amylase.

## Appendix I.

In order to derive eq. 1:

$$r_l = \frac{k_a}{k_d} \{[N]e^{-k_h t}\}^{n_c} \quad (1)$$

the kinetic model of nucleation step is commonly described as an  $n_c$ -order reaction with respect to the free monomer concentration  $c$  with the rate  $r$  shown below (eq. 2)<sup>[11]</sup>:

$$r = k_n c^{n_c} \quad (2)$$

where  $k_n$  is the nucleation rate constant, and  $n_c$  is an effective reaction order of nucleation. When the aggregates formed, they were unstable and had an increased probability of dissociating back to monomers. As result, the  $k_n$  could be decribed as the ratio of the association rate constant  $k_a$  to the dissociation rate constant  $k_d$ , as shown below (eq. 3):

$$k_n = \frac{k_a}{k_d} \quad (3)$$

In the hydrolysis process, the cleaved short polypeptide species are the building blocks for the amyloid fibrils, and thus defined as monomers. Obviously, such monomer concentration closely depends on the hydrolysis kinetics (eq. 4)<sup>[12]</sup>:

$$c = [N]e^{-k_h t} \quad (4)$$

where  $c$  is the monomer concentration,  $[N]$  is the initial concentration of native protein,  $k_h$  is the hydrolysis rate constant, and  $t$  is reaction time. According to eq. 2-4, leading to eq. 1.

## References

- [1] K. Yu, J. Yang, Y. Y. Zuo, *Langmuir* **2016**, *32*, 4820.
- [2] R. P. Valle, T. Wu, Y. Y. Zuo, *ACS Nano* **2015**, *9*, 5413.
- [3] T. Zako, M. Sakono, N. Hashimoto, M. Ihara, M. Maeda, *Biophys. J.* **2009**, *96*, 3331.
- [4] E. V. Hackl, J. Darkwah, G. Smith, I. Ermolina, *Eur. Biophys. J.* **2015**, *44*, 249.
- [5] O. K. Gasymov, B. J. Glasgow, *Biochim. Biophys. Acta.* **2007**, *1774*, 403.
- [6] D. Wang, Y. Ha, J. Gu, Q. Li, L. Zhang, P. Yang, *Adv. Mater.* **2016**, *28*, 7414.
- [7] X. M. He, D. C. Carter, *Nature* **1992**, *358*, 209.
- [8] D. I. Cattoni, S. B. Kaufman, F. L. G. Flecha, *Biochim. Biophys. Acta.* **2009**, *1794*, 1700.
- [9] D. M. Togashi, A. G. Ryder, *J. Fluoresc.* **2008**, *18*, 519.
- [10] B. Ahmad, M. Z. Ahmed, S. K. Haq, R. H. Khan, *Biochim. Biophys. Acta.* **2005**, *1750*, 93.
- [11] A. Šarić, T. C. T. Michaels, A. Zacccone, T. P. J. Knowles, D. Frenkel, *J. Chem. Phys.* **2016**, *145*, 211926.
- [12] A. Kroes-Nijboer, P. Venema, J. Bouman, van der Linden, *Langmuir* **2011**, *27*, 5753.